

Holography of time machines

Roberto Emparan^{a,b} and Marija Tomašević^b

^a*Institució Catalana de Recerca i Estudis Avançats (ICREA), Passeig Lluís Companys 23, E-08010 Barcelona, Spain*

^b*Departament de Física Quàntica i Astrofísica, Institut de Ciències del Cosmos, Universitat de Barcelona, Martí i Franquès 1, E-08028 Barcelona, Spain*

E-mail: emparan@ub.edu, mtomasevic@icc.ub.edu

ABSTRACT: We use holography to examine the response of quantum fields to the appearance of closed timelike curves in a dynamically evolving background that initially does not contain them. For this purpose, we study a family of two-dimensional spacetimes that model very broad classes of wormhole time machines. The behavior of conformal theories in these spacetimes is then holographically described by three-dimensional AdS bulk geometries that we explicitly construct. The dual bulk spacetime is free from any divergences, but splits into two disconnected components, without and with CTCs, which are joined only through the boundary; this implies that passages across the chronology horizon are impossible for observers with finite energy. The bulk region with CTCs is a geodesically incomplete spacetime. Therefore, the bulk enforces the chronology protection principle in the most explicit manner – by completely separating the pathological part from the rest of the spacetime.

Contents

1	Introduction	1
2	Building intuition: Misner spacetimes	3
2.1	Constant time shift: the tilted cylinder	3
2.2	Growing time shift: Misner-AdS spacetime	3
2.3	Flat limit: Misner spacetime	8
2.4	Energy gain in the time machine	8
3	Holographic dual of the time machine	9
3.1	Stress tensor	9
3.2	Bulk metric and regularity	10
4	Patching up the bulk geometry	13
4.1	$\alpha > 1/2$: Split-bulk chronology protection	13
4.2	$\alpha < 1/2$: Thermal censorship	15
5	Bulk dual for flat Misner spacetime	16
6	A stress-free time machine is dual to a bulk wormhole	17
7	Euclidean analysis	18
8	Time machines from wormholes	20
9	Discussion	22
A	Hyperboloidal embeddings	24
B	Bulk reconstruction in AdS_3	26
C	Mapping the flat-Misner bulk to Poincaré AdS_3	27

1 Introduction

Time machines, or spacetimes with closed timelike curves (CTCs), are infamous for their often unpleasant and paradoxical consequences. Yet, it has never been fully clarified whether they necessarily contradict the known laws of physics. Various no-go theorems exist which, under physically plausible assumptions, deem the operation of a time machine impossible. For instance, the achronal average null energy condition excludes the possibility of time

machines [1] simply by incompatibility. Nevertheless, studying spacetimes that develop CTCs can uncover certain aspects of the laws of physics that are not manifest otherwise.

In this paper, we will be interested in studying if and how quantum effects play a role in time machine spacetimes. Such effects have been studied earlier, most notably in [2–5], from which the “chronology protection conjecture” was developed. In a nutshell, the conjecture states that quantum gravity forbids the creation of closed timelike curves. Such a statement is not without its evidence, given that several calculations have shown a divergence of a quantum stress tensor at the chronology (Cauchy) horizon¹. Moreover, one can show that semiclassical Einstein’s equations fail to hold for particular points on the chronology horizon, thereby promptly invoking the need for a resolution within quantum gravity [7, 8]².

It is then natural to explore chronology protection within the context of AdS/CFT. The study will throw light on the importance of strong coupling in the quantum response to an attempt to create a time machine. Furthermore, we may get a dual geometric view of the mechanism that forbids the passage across the chronology horizon into the CTC region of the spacetime.

For this purpose, we will consider a broad class of generic two-dimensional spacetimes with CTCs, and reconstruct the bulk that is dual to the conformal fields in such spacetimes. Therefore, the boundary spacetime will exhibit the known features of time machines (such as the aforementioned stress tensor divergence). However, the novelty lies in the peculiar way that the bulk upholds the chronology protection. In particular, we will show that no finite energy excitations can ever cross to the CTC-region; such a conclusion is robust – not because of any singularity, since the AdS₃ bulk has constant curvature – but due to the fact that the bulk fragments into two disconnected components, which are joined only through the boundary. The location of the chronology horizon will then sit on the boundary of the spacetime, making any bulk passages impossible for observers with finite energy. Moreover, we will show that the CTC-region becomes geodesically incomplete for all states of the boundary time machine, as the notion of global hyperbolicity fails to persist. Such incompleteness then leads to interesting holographic interpretations, since the bulk reconstruction becomes incomplete as well.

The paper is organized as follows: we introduce in Sec. 2 a simple, intuitive toy model for a time machine spacetime, given by the Misner-AdS geometry; in Sec. 3, we construct the bulk dual geometry from the AdS₂ boundary spacetime, and we discuss its numerous features, including the geometric way in which chronology protection is implemented; we continue with the analysis of the bulk geometry in Sec. 4, and we classify the different states of the boundary CFT; in Sec. 5, we obtain the dual geometry for a flat Misner spacetime; Sec. 6 analyzes a special state of the CFT whose holographic dual is a bulk wormhole; in Sec. 7, we perform a Euclidean analysis in order to determine the preferred state of the

¹The chronology horizon exists in spacetimes in which we have localized creation of CTCs. If we had started with a spacetime that has CTCs at every point, there would be no room for chronology protection; such setups were studied in a holographic setup in [6].

²However, one can see that this need not be the case for self-consistent spacetimes which incorporate the gravitational effect of the quantum fields, as we will show elsewhere.

boundary theory after a time machine has formed; in Sec. 8 we discuss how the same AdS₂ time machine spacetime naturally emerges in wormhole setups, and how our results affect the physics of such traversable wormholes; we finish in Sec. 9 and we discuss the possible future directions; in App. A, we present embeddings of the geometries that we study; in App. B, we review the bulk reconstruction procedure for AdS₃ and apply it to our problem; App. C presents a map of one of our bulk geometries to Poincaré-AdS₃, which complements the ones given in the main text.

2 Building intuition: Misner spacetimes

We will now discuss a simple model of a time machine that shows many of its features in a very clear and appealing manner. It admits straightforward generalizations to higher dimensions, given in, e.g. [9].

2.1 Constant time shift: the tilted cylinder

As a preliminary, consider a ‘tilted cylinder’ spacetime. The metric

$$ds^2 = -(d\tau + v d\psi)^2 + d\psi^2, \quad (2.1)$$

with constant v is locally flat space, as one can see by changing

$$\tau = t - v\psi. \quad (2.2)$$

If we identify

$$\psi \sim \psi + L \quad (2.3)$$

at constant τ , this amounts to identifying

$$\psi \sim \psi + L, \quad t \sim t + vL. \quad (2.4)$$

We can think of the spatial circle as the loop threading a wormhole, and then (2.4) indicates that the mouths are connected with a constant time delay $\Delta t = vL$. It can also be seen as the result of making identifications along the circle in a frame where the circle is moving with velocity v .

As long as $0 \leq v < 1$ the identification is along a spacelike direction, and the spacetime (2.1) is not a time machine.

2.2 Growing time shift: Misner-AdS spacetime

Now we build a cylinder with a tilt v that grows linearly in time, with acceleration a (see Fig. 1) so that

$$ds^2 = -(d\tau + a\tau d\psi)^2 + d\psi^2. \quad (2.5)$$

When we do this, the geometry is no longer flat space, but instead AdS₂ with radius $1/a$. This can be seen by changing

$$t = \tau e^{a\psi}, \quad x = \frac{1}{a} e^{a\psi}, \quad (2.6)$$

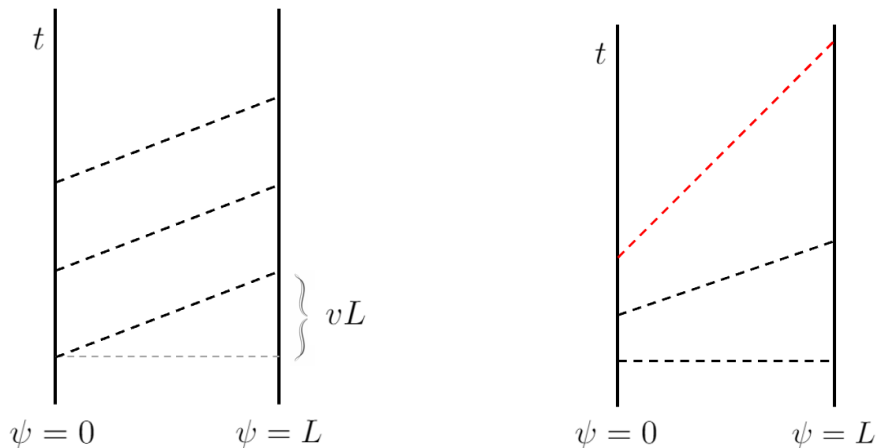


Figure 1: **Left:** Tilted cylinder with $v = \text{const}$. The sides $\psi = 0$ and $\psi = L$ are identified along the dashed lines, at the same time τ but different time t . **Right:** Misner-AdS₂ cylinder with linearly increasing $v = a\tau$. The red line indicates that lightlike-separated points are identified, and therefore a closed null curve is present. At later times, closed timelike curves appear.

i.e.,

$$\tau = \frac{t}{x}, \quad \psi = \frac{1}{a} \ln ax, \quad (2.7)$$

so the metric becomes AdS₂ in Poincaré coordinates,

$$ds^2 = \frac{-dt^2 + dx^2}{a^2 x^2}. \quad (2.8)$$

Notice that $\psi \in (-\infty, +\infty)$ covers the entire Poincaré patch $x \in (0, \infty)$. But we are interested in making ψ into a circle, identifying it periodically along lines of constant τ , i.e.,

$$(\tau, \psi) \sim (\tau, \psi + L). \quad (2.9)$$

With this identification, the geometry (2.5) is known as the Misner-AdS₂ spacetime [9]. Writing the metric as

$$ds^2 = -d\tau^2 - 2a\tau d\psi d\tau + (1 - a^2\tau^2)d\psi^2 \quad (2.10)$$

makes clear that $\partial/\partial\psi$ becomes timelike, and hence CTCs appear, when

$$|\tau| > \frac{1}{a}. \quad (2.11)$$

There are two regions with CTCs, one in the future and another in the past, separated from the non-CTC region by respective chronological horizons $\tau = \pm 1/a$. Our intention is to view this as model for a spacetime that starts at $\tau = 0$ without any CTCs, and then evolves a growing time shift until it becomes a time machine. We will not be much interested in the time machine in the past, but our results readily extend to it.

Up to an overall scale, the only parameter of the geometry is the dimensionless number

$$\Delta = aL. \quad (2.12)$$

It measures the increase rate of the tilting (or redshifting rate) in units of the circle length. For fixed circle length, having small acceleration, i.e., slow redshifting, is equivalent to small Δ . Instead, in the following we will fix the AdS radius to one, i.e.,

$$a = 1, \quad L = \Delta, \quad (2.13)$$

so that reducing Δ shrinks the circle length. However, we will still refer to $\Delta \ll 1$ as the *slow time machine* limit.

We should also note that (2.8), with the identification of points

$$(t, x) \sim e^\Delta(t, x) \quad (2.14)$$

implied by (2.9), is exactly the geometry that one finds in a wormhole time machine model spacetime where time runs at different rates near each of the two mouths, as we will see in Sec. 8. The fundamental region can be chosen in many ways, but a convenient one is (see Fig. 2)

$$x \in (1, e^\Delta), \quad t \in (-\infty, \infty), \quad (2.15)$$

and at the region boundaries the coordinates jump as in

$$(t, 1) \sim (e^\Delta t, e^\Delta). \quad (2.16)$$

A convenient representation is obtained working in the null coordinates x^\pm , given by

$$x^- = t - x, \quad x^+ = t + x, \quad (2.17)$$

so that

$$ds^2 = -\frac{4}{(x^+ - x^-)^2} dx^+ dx^-, \quad (2.18)$$

and the identifications are

$$x^\pm \sim e^\Delta x^\pm. \quad (2.19)$$

A convenient fundamental region (different than (2.15)) is³

$$x^+ \in (1, e^\Delta), \quad x^- < x^+, \quad (2.20)$$

(the latter is equivalent to $x > 0$) with boundary conditions

$$(1, x^-) \sim (e^\Delta, e^\Delta x^-). \quad (2.21)$$

The geometry has a Killing vector

$$k = \frac{\partial}{\partial \psi} = t \frac{\partial}{\partial t} + x \frac{\partial}{\partial x} = x^+ \frac{\partial}{\partial x^+} + x^- \frac{\partial}{\partial x^-}, \quad (2.22)$$

³This is for positive times. For negative ones, we take $x^- \in (-e^\Delta, -1)$.

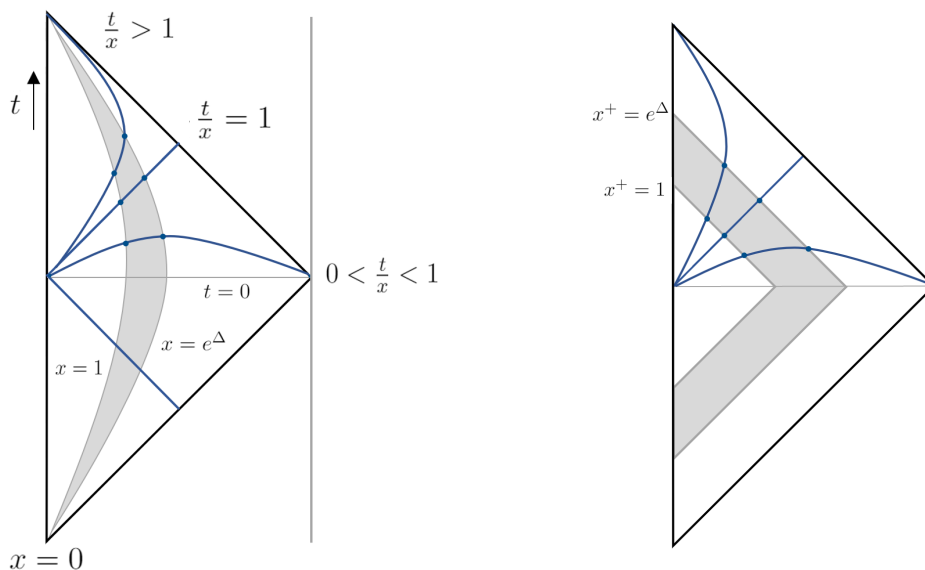


Figure 2: Different choices for the fundamental region of the Misner-AdS₂ spacetime (shaded in gray) when embedded in the Poincaré-AdS₂ half-diamond, (2.8) or (2.18). Blue dots indicate identified points, compactifying the gray strip into a cylinder. The identifications are along a light ray at the chronological horizon $t/x = 1$, and along timelike curves in the upper wedge $t/x > 1$, and along spacelike slices in $t/x < 1$. **Left:** The fundamental region is given in terms of (t, x) coordinates, as in (2.15). **Right:** The fundamental region is defined through x^\pm coordinates, as in (2.20).

whose orbits are periodic under the identifications we are making. These same identifications break other symmetries of AdS₂, in particular the time translation symmetry generated by $\partial/\partial t$. As a result, the geometry is time-dependent in a manner made manifest by the growing tilt of the Misner-AdS cylinder.

Finally, let us present another set of coordinates in which the metric becomes diagonal but in a different form than (2.8). Namely, keep τ but change $\psi \rightarrow \phi$ so that

$$d\psi = d\phi + \frac{\tau}{1 - \tau^2} d\tau, \quad (2.23)$$

i.e.,

$$\psi = \phi - \ln \sqrt{|1 - \tau^2|}. \quad (2.24)$$

The metric of Misner-AdS₂ now becomes

$$ds^2 = -(\tau^2 - 1)d\phi^2 + \frac{d\tau^2}{\tau^2 - 1} \quad (2.25)$$

with periodic $\phi \sim \phi + \Delta$ along the orbits generated by the Killing vector

$$k = \frac{\partial}{\partial \phi}. \quad (2.26)$$

The form of the metric is like Rindler-AdS₂, but in the latter, conventionally one considers the region $\tau^2 > 1$, so that τ is a spatial coordinate and ϕ is the time. Therefore Misner-AdS₂ is Rindler-AdS₂ with closed timelike orbits, and the Rindler acceleration horizons $\tau = \pm 1$ correspond to the chronology horizons of the Misner space. In the CTC region, the spatial sections are non-compact. The non-CTC region $\tau^2 < 1$ is time-dependent with circular spatial sections. It is a Milne-AdS₂ cosmology⁴ that is spatially compact but is free of CTCs.

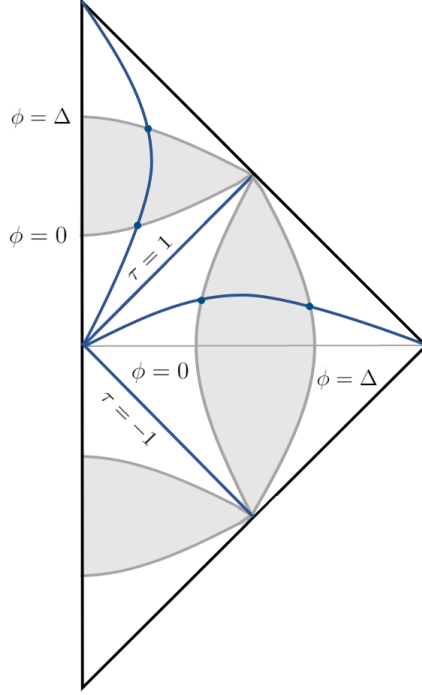


Figure 3: The fundamental regions for the lower and upper patches in (τ, ϕ) coordinates, both shaded in gray. The blue dots correspond to identified points. **Lower patch:** Determined by $\tau^2 < 1$, $\phi \in [0, \Delta]$. Blue line is $\tau = \text{const} < 1$ slice. **Upper patch:** Described with $\tau > 1$, and with $\phi \in [0, \Delta]$ now as compact time coordinate. Blue line indicates $\tau = \text{const} > 1$ trajectory. The chronology horizons are reached for $\tau = \pm 1$.

In these coordinates the CTC and non-CTC regions are described as separate coordinate patches. We will refer to the region $\tau > 1$ as the ‘upper patch’ and to $-1 < \tau < 1$ as the ‘lower patch’. Although there is also a past CTC region for $\tau < -1$, we will mostly ignore it in our discussion.

⁴The Milne universe is a cosmology obtained as a wedge of Minkowski space that either expands or collapses. Milne-AdS₂ is a bouncing universe that first expands and then collapses.

2.3 Flat limit: Misner spacetime

Let us now zoom in on the geometry near the (future) chronological horizon at $\tau = 1$. To this effect, we make

$$\tau = 1 + \epsilon T, \quad (2.27)$$

where T is a new coordinate and rescale the metric such that in the limit $\epsilon \rightarrow 0$, (2.5) becomes

$$\epsilon^{-1} ds^2 \rightarrow -2dTd\psi - 2Td\psi^2. \quad (2.28)$$

When ψ is a periodic coordinate, this is the geometry of Misner space as originally introduced in [10]. It is a discrete quotient of Minkowski space that contains CTCs when $T > 0$. This structure is inherited from the original Misner-AdS spacetime. We can also obtain the limit in the null coordinates (2.17) by taking

$$x^+ = -\frac{2}{X^+}, \quad x^- = \frac{\epsilon}{2} X^-, \quad (2.29)$$

such that (2.18) becomes

$$\epsilon^{-1} ds^2 \rightarrow -dX^+ dX^-. \quad (2.30)$$

This is made into a time machine when we identify along Minkowski boosts,

$$X^+ \sim e^{-\Delta} X^+, \quad X^- \sim e^{\Delta} X^-. \quad (2.31)$$

The geometry is contained in the half-space $X^+ < 0$, and the non-CTC and CTC regions correspond to $X^- < 0$ and $X^- > 0$, respectively, with chronological horizon at $X^- = 0$.

The identification (2.31) allows to present Misner space as a model of the time machine that results when the two mouths of a wormhole approach and pass by each other with relative velocity $\tanh \Delta$. Although flat Misner space is slightly simpler than Misner-AdS, the latter is of interest to us not as a more general class of spacetimes that evolve CTCs, and the model of a broad family of wormhole time machines, as we argue in Sec. 8.

2.4 Energy gain in the time machine

By analyzing geodesic motion in the previous spacetimes, one easily sees that a particle on the circle, even if it starts at rest, will acquire an increasing non-zero velocity. The particle gains more and more energy by ‘falling’ inside the circle due to its tilting. In the Poincaré representation (2.8), when the particle falls to $x = e^{\Delta}$, the identifications (2.16) lift it up in the gravitational field to $x = 1$. In the flat Misner spacetime, the energy gain is due to Lorentz boosting. For each turn around the circle, the energy of the particle increases by a factor e^{Δ} . When the time machine is about to form, the energy gain diverges.

When we put a quantum CFT in this spacetime, its fluctuations will gain energy in the same manner. This is natural, since the field will be excited by the time dependence of the geometry. The CFT on a circle has a gap $2\pi/L$. When a is small, i.e., $\Delta < 2\pi$, the CFT will not get much excited, at least initially, although effects will build up over a time scale $\sim 1/a$, when the spacetime is about to become a time machine. When a is large, $\Delta > 2\pi$, the time dependence will be able to excite the CFT much more efficiently from early on. Although these arguments might lead us to expect a qualitative change in the behavior of the CFT when $\Delta \sim 2\pi$, we will only find very limited differences in its dependence on Δ .

3 Holographic dual of the time machine

After characterizing the geometry of the time machine spacetime, we now turn to the evolution of quantum fields in it. We employ the holographic approach in which a strongly coupled conformal field theory with large central charge c is described through a dual three-dimensional bulk geometry with the Misner-AdS₂ geometry at its boundary.

3.1 Stress tensor

In order to reconstruct this bulk, we first constrain the form of the CFT stress tensor. For a CFT, it can be decomposed into a traceless component and an anomalous trace term

$$\langle T_{ij} \rangle = \langle \hat{T}_{ij} \rangle + \frac{c}{48\pi} R g_{ij} \quad (3.1)$$

with

$$\langle \hat{T}^i{}_i \rangle = 0, \quad R = -2, \quad (3.2)$$

the latter being the scalar curvature of unit-radius AdS₂. Our goal is to obtain the traceless part $\langle \hat{T}_{ij} \rangle$.

Conformal invariance, together with the time-reversal symmetry of the background geometry, impose that the stress tensor, in the null coordinates of (2.18), takes the form

$$\langle \hat{T}_{ij} \rangle dx^i dx^j = -\alpha \frac{c}{24\pi} \left(\left(\frac{dx^+}{x^+} \right)^2 + \left(\frac{dx^-}{x^-} \right)^2 \right), \quad (3.3)$$

with a coefficient α that, in principle, can be a function of the coordinates. However, the translation symmetry along ψ leaves only the possibility that it is a function of t , and then the covariant conservation condition $\nabla_i \langle \hat{T}^{ij} \rangle = 0$ requires that α be constant.

In (τ, ϕ) coordinates, the stress tensor is diagonal,

$$\langle \hat{T}_{ij} \rangle dx^i dx^j = -\alpha \frac{c}{12\pi} \left(d\phi^2 + \frac{d\tau^2}{(1 - \tau^2)^2} \right), \quad (3.4)$$

and therefore does not have any energy-flow component. Thus, these coordinates are adapted to a frame comoving with the CFT. In this frame, when $\tau^2 < 1$ and ϕ is a spatial direction, the stress tensor is time-dependent but spatially homogeneous. When $\tau^2 > 1$ and ϕ is timelike and τ spacelike, the stress-tensor it is static but inhomogeneous.

Our strategy now is to employ the standard bulk reconstruction procedure [11] in order to obtain an exact solution of the three-dimensional Einstein-AdS equations that has the Misner-AdS₂ geometry at its boundary, and (3.3) as its holographic stress tensor. This construction yields a local solution for every value of α , but α should not be a free parameter. We expect that the ground state of the CFT, and its stress tensor, is determined by the geometry where it propagates, and this should also be a feature of the bulk geometry with a given fixed boundary. In the present case, α must be a function of Δ . In typical AdS/CFT fashion, the relation will follow after imposing a regularity condition in the bulk.

3.2 Bulk metric and regularity

In App. B, we explain the procedure of bulk reconstruction in AdS₃/CFT₂, and apply it to the Misner-AdS₂ time machine spacetime with stress tensor (3.3). In the null coordinates of (2.18), the bulk metric that we obtain takes the form

$$ds^2 = \frac{\ell^2}{z^2} \left[dz^2 - \left(\left(1 + \frac{z^2}{4} \right)^2 \frac{4}{(x^+ - x^-)^2} + \frac{\alpha^2}{16} \left(\frac{1}{x^+} - \frac{1}{x^-} \right)^2 z^4 \right) dx^+ dx^- \right. \\ \left. - \alpha \frac{z^2}{2} \left(1 + \frac{z^2}{4} \right) \left(\left(\frac{dx^+}{x^+} \right)^2 + \left(\frac{dx^-}{x^-} \right)^2 \right) \right]. \quad (3.5)$$

The coordinate z extends from the boundary at $z = 0$ into the bulk with $z > 0$, in a manner that we will explore in detail below. Some expressions become simpler in terms of the proper distance $\sigma = \ln(2/z)$, and we will use it occasionally.

We can also transform (3.5) into any of the coordinates for the boundary metric introduced in the previous section. In the coordinates (τ, ϕ) it becomes a diagonal metric,

$$ds^2 = \frac{\ell^2}{z^2} \left[dz^2 - \left(1 + \frac{z^2}{4} + \frac{\alpha}{2} \frac{z^2}{1 - \tau^2} \right)^2 \frac{d\tau^2}{1 - \tau^2} + \left(1 + \frac{z^2}{4} - \frac{\alpha}{2} \frac{z^2}{1 - \tau^2} \right)^2 (1 - \tau^2) d\phi^2 \right]. \quad (3.6)$$

Recall that τ is timelike and ϕ spacelike when $\tau^2 < 1$, and they reverse roles when $\tau^2 > 1$. It is easy to see that curves of constant τ and constant ϕ are geodesic.

This geometry is, by construction, locally AdS₃ for any value of α , but global bulk regularity is not guaranteed. To begin the interpretation of the geometry, note that the boundary metric and the CFT stress tensor are independent of ϕ , and therefore

$$k = \frac{\partial}{\partial \phi} \quad (3.7)$$

is also a Killing vector of the bulk. Its norm is given by

$$|k|^2 = g_{\phi\phi} = \frac{\ell^2}{z^2} \frac{1}{1 - \tau^2} \left((1 - \tau^2) \left(1 + \frac{z^2}{4} \right) - \frac{\alpha}{2} z^2 \right)^2, \quad (3.8)$$

which implies that k is spacelike for $|\tau| < 1$ and timelike for $|\tau| > 1$. The bulk then contains CTCs in precisely the same range of τ as in the boundary. However, when $|\tau| = 1$ the vector k is null only when $z = 0$. At any finite distance z inside the bulk, k diverges when $|\tau| = 1$. Therefore, the chronological horizon is only present at the boundary.

There are, however, points in the bulk where $|k| = 0$ without k being null. This happens where

$$z = z_{\max} = 2\sqrt{\frac{1 - \tau^2}{2\alpha - 1 + \tau^2}}. \quad (3.9)$$

As will become apparent presently, we are mostly interested in values of α in the range

$$\alpha > \frac{1}{2}, \quad (3.10)$$

so that z_{\max} is real when $|\tau| < 1$. Then, when $0 < z < z_{\max}$ the vector k is spacelike, and it has a fixed point-set at $z = z_{\max}$. The absence of conical singularities at these points demands that we fix the periodicity Δ of the orbits of k to the value

$$\Delta = \lim_{|k| \rightarrow 0} \frac{2\pi}{(\partial_\mu |k| \partial^\mu |k|)^{1/2}} = \frac{2\pi}{\sqrt{2\alpha - 1}}, \quad (3.11)$$

or, equivalently,

$$\alpha = \frac{1}{2} + \frac{2\pi^2}{\Delta^2}. \quad (3.12)$$

The condition (3.10) then follows whenever $\Delta \neq 0$.

Values of α outside the range (3.10) may yield sensible bulks as long as there are no fixed points of k in the region $\tau^2 < 1$ where it is spacelike. This happens when $\alpha \leq 0$. However, these states have non-negative energy and therefore the state at $\tau = 0$ does not start in its ground state with the negative Casimir energy of the CFT in a circle. In the lower patch, before CTCs form, we will then consider that α is given by (3.12), as the only values that correspond to the physical process of time machine formation that we want to investigate.

When $\alpha < 0$ the stress tensor is that of a thermal state, and we expect a horizon in the bulk. Indeed, in the region $\tau^2 > 1$ a Killing horizon appears at

$$z = z_{\text{hor}} = 2\sqrt{\frac{\tau^2 - 1}{2|\alpha| + 1 - \tau^2}}, \quad \alpha < 0, \quad (3.13)$$

since at these points the timelike vector k becomes null. We will revisit the properties of this horizon in Sec. 4. In the range of $0 < \alpha \leq 1/2$ conical singularities are unavoidable for some range of $\tau^2 < 1$ if $\Delta \neq 0$. These values of α therefore do not yield acceptable states.

The state with $\alpha = 0$ also starts out excited above the Casimir negative-energy state, but it has an interesting interpretation that we will discuss in Sec. 6.

This completes the bulk construction, at least as long as we are only concerned with the regime before CTCs are developed. We have obtained that stress tensor in the ground state of the strongly coupled CFT in the Misner-AdS₂ geometry, with a given shifting rate Δ , and for times $|\tau| < 1$, has traceless component

$$\langle \hat{T}_{ij} \rangle dx^i dx^j = -c \left(\frac{1}{48\pi} + \frac{\pi}{12\Delta^2} \right) \left(\left(\frac{dx^+}{x^+} \right)^2 + \left(\frac{dx^-}{x^-} \right)^2 \right), \quad (3.14)$$

where the central charge is $c = 3\ell/2G$. We omit the trace part since it is simply the Weyl anomaly in AdS₂, which has no consequences of interest to us.

Comparison with free CFT. The dependence on Δ differs, as would be expected, from the one obtained in [5] for a free conformal scalar field, given by

$$\langle \hat{T}_{ij} \rangle dx^i dx^j = -F(\Delta) \left(\left(\frac{dx^+}{x^+} \right)^2 + \left(\frac{dx^-}{x^-} \right)^2 \right),$$

where

$$F(\Delta) = \frac{1}{8\pi} \sum_{n=1}^{\infty} \frac{1}{\sinh^2(n\Delta/2)}.$$

The analysis of $F(\Delta)$ is simpler if we rewrite the sum in terms of q-trigamma functions, but one can already see some of its distinct features in its current form. First, let us note that the two functions match exactly for small values of Δ if we consider a number c of conformal scalar fields: this is the regime of the “slow time machine”, in which the effects can be captured perturbatively in both cases. However, for large values of Δ , the function $F(\Delta)$ falls off exponentially to zero; large Δ corresponds to strong time machine effects. We see that this behaviour is quite different compared to our case, where for large Δ we obtain a constant contribution, as can be seen from (3.14). Therefore, the strong coupling contributes to a larger field excitation for fast time machine formation, compared to the free field analysis.

“Slow time machine” regime. Let us focus on the initial, small redshifting regime. For this purpose, we focus on times shortly after $\tau = 0$, rescale ψ to keep the circle length finite, and also rescale z , whose range shrinks for small Δ (i.e., large α). All of this is achieved by changing

$$(\tau, \psi, z) \rightarrow \frac{\Delta}{2\pi}(\tau, \psi, z), \quad (3.15)$$

and then expanding for small Δ . Observe that the new ψ has periodicity 2π . If we furthermore introduce, for mere convenience, the proper bulk distance coordinate $\sigma = \ln(2/z)$, then the bulk geometry becomes

$$ds^2 = d\sigma^2 - \cosh^2 \sigma d\tau^2 + \sinh^2 \sigma d\psi^2 - \frac{\Delta}{\pi} \tau \sinh^2 \sigma d\tau d\psi + O(\Delta^2), \quad (3.16)$$

for which the holographic stress tensor is

$$\langle T_{ij} \rangle dx^i dx^j = -\frac{c}{24\pi} \left(d\tau^2 + d\psi^2 - \frac{2\Delta}{\pi} \tau d\tau d\psi + O(\Delta^2) \right) \quad (3.17)$$

(the anomalous trace vanishes to linear order in Δ). The leading order geometry in (3.16) is the global AdS_3 spacetime, which is the bulk dual of the CFT in a circle with Casimir energy $\langle T_{tt} \rangle = \langle T_{\psi\psi} \rangle < 0$. The correction to the metric proportional to Δ gives the bulk dual of the energy flux $\langle T_{t\psi} \rangle$ that is created by the growing tilt in the Misner- AdS_2 cylinder.

In the interpretation of Sec. 8, the geometry (3.16) captures holographically the quantum effects induced when beginning to create a time differential between the two mouths of a wormhole.

Geometric chronology protection. Observe that (3.9) implies that as τ increases from $\tau = 0$ towards the chronological horizon at $\tau = 1$, the value of z_{\max} decreases: The extent of the bulk away from the boundary shrinks, until the moment $\tau = 1$ when the bulk size vanishes. Then, continuing to $\tau > 1$, the bulk reappears, and indeed there is no maximum value of z anymore, since z can run from 0 to ∞ . Below we will further clarify what is going on in this peculiar geometry, but for now let us emphasize one important consequence of the closing up of the bulk at $|\tau| = 1$:

It is impossible to cross between the chronologically normal region and the time machine region, while remaining a finite distance inside the bulk.

Or, in dual terms:

An excitation of the CFT with finite energy density cannot cross the chronological horizon.

4 Patching up the bulk geometry

For any value of α , the bulk metric that we have constructed is locally equivalent to AdS_3 , and therefore it must be possible to find a change of coordinates that transforms it into other more familiar forms of AdS_3 .

4.1 $\alpha > 1/2$: Split-bulk chronology protection

We have argued that, at least when $\tau^2 < 1$, we must fix α in terms of Δ as in (3.12). The identifications are then along the orbits of a spacelike isometry $k = \partial/\partial\phi$ with a rotational fixed point. These are also features of global AdS_3 when we write it in the form⁵

$$ds^2 = -(r^2 + 1)dt^2 + \frac{dr^2}{r^2 + 1} + r^2 d\phi^2, \quad (4.1)$$

with $\phi \sim \phi + 2\pi$. We then identify φ with an appropriately rescaled ϕ , and equate r^2 with the norm of k . A straightforward integration then allows us to obtain t as a function of (τ, z) , to find that

$$\varphi = \frac{2\pi}{\Delta}\phi, \quad (4.2)$$

$$r^2 = \left(\frac{\Delta}{2\pi}\right)^2 \frac{1 - \tau^2}{z^2} \left(1 + \frac{z^2}{4} - \frac{\alpha}{2} \frac{z^2}{1 - \tau^2}\right)^2, \quad (4.3)$$

$$t = \frac{\pi}{\Delta} \ln \left| \frac{1 + \tau}{1 - \tau} \right| - \arctan \frac{z^2 + \left(\frac{\Delta}{\pi}\right)^2 \left(1 - \tau^2 - \frac{z^2}{4}\tau^2\right)}{\frac{\Delta}{\pi} z^2 \tau} + \frac{\pi}{2} \text{sgn } \tau, \quad (4.4)$$

correctly maps (4.1) onto (3.6) when α given by (3.12). We have added a term to make t continuous at the change in branch of \arctan when $\tau = 0$. This map is indeed valid for both $\tau^2 < 1$ and $\tau^2 > 1$, but the way that global AdS_3 is covered is different in each patch.

Lower patch. One can see that for any fixed z , the coordinate t is a continuous and monotonous function of τ in the entire range $\tau \in (-1, +1)$. Also, r runs continuously in $[0, \infty)$ when $z \in (0, z_{\max}]$. Then the lower patch of (3.6) covers global AdS_3 in one-to-one fashion. In other words, the lower patch bulk is a geodesically complete spacetime.

One may ask how the static bulk of global AdS_3 is compatible with the time-dependence of the boundary geometry. The answer is that the timelike Killing vector in the bulk does not generate time translations at the boundary, since these are broken by the asymptotic boundary conditions. This is in fact what allows the boundary geometry to cover the two patches, while they remain disconnected through the bulk.

⁵Henceforth we set the AdS_3 radius $\ell = 1$.

Upper patch. The upper patch contains CTCs since there the coordinate ϕ is timelike and is periodically identified. We see that in this region the change of coordinates (4.3) makes $r^2 < 0$, and indeed, as we will presently see, $r^2 < -1$. It is then convenient to rename coordinates as

$$t = \bar{\varphi}, \quad \varphi = \bar{t}, \quad r^2 = -(\bar{r}^2 + 1), \quad (4.5)$$

so (4.1) becomes

$$ds^2 = -(\bar{r}^2 + 1)d\bar{t}^2 + \frac{d\bar{r}^2}{\bar{r}^2 + 1} + \bar{r}^2 d\bar{\varphi}^2. \quad (4.6)$$

Let us emphasize that this renaming is just a convenience for clarity. The map between (3.6) and (4.6) is simply the same as above, after renaming coordinates. Now the Killing symmetry of (3.6) corresponds to the timelike isometry $\partial/\partial\bar{t}$. Since this implies that $\bar{t} \sim \bar{t} + 2\pi$, the geometry is like that of global AdS₃ in the hyperboloidal embedding (see App. A), before one unwraps the time direction to obtain the universal cover.

The change of coordinates for \bar{r} can be written in the form

$$\bar{r}^2 = \left(1 + \frac{\left(\frac{\Delta}{\pi}\sqrt{\tau^2 - 1} - z\right)^2 + \left(\frac{\Delta}{2\pi}\right)^2 z^2 \tau^2}{2\frac{\Delta}{\pi}z\sqrt{\tau^2 - 1}} \right)^2 - 1. \quad (4.7)$$

This shows that $\bar{r}^2 > 0$ strictly: *the coordinates in the upper patch never get to $\bar{r} = 0$* . It turns out that the function $\bar{r}(\tau, z)$ takes its minimum value for

$$z \rightarrow 0, \quad \tau^2 \rightarrow 1, \quad \frac{z^2}{\tau^2 - 1} = \frac{2}{\alpha} = \frac{\left(\frac{\Delta}{\pi}\right)^2}{1 + \left(\frac{\Delta}{2\pi}\right)^2}, \quad (4.8)$$

where

$$\bar{r}_{\min} = \frac{\Delta}{2\pi} \quad (4.9)$$

is achieved. So there is a *hole* in the patch; in other words, the bulk in the upper patch becomes geodesically incomplete. Its geometry is that of global AdS₃, with periodic time, and with a hole of radius \bar{r}_{\min} in its middle.

Let us note a couple of things about this patch. First, the function $|\phi(\tau, z)|$ also has a minimum, but in this case it does not matter. Since $\phi(\tau, z)$ extends to arbitrarily large values, it can cover all angles in the circle in an infinite number of covers. Second, the way in which the (τ, z) coordinates cover global AdS₃ is a very intricate, infinite multiple cover. Finally, the periodicity in the upper patch is enforced by gluing it to the lower patch. However, the gluing happens only at the boundary, indicating that the bulk patches are *completely disconnected*.

Additionally, all the Δ dependence is in the coordinate changes: the two AdS₃ bulks, lower and upper, are independent of Δ , not only locally but also globally, in the sense that no Δ -dependent identifications are made. The distinction in the bulks for different time machines lies in the regions of the bulk that are covered in each case, and then this only happens in the upper patch, with a hole of radius $\Delta/2\pi$.

4.2 $\alpha < 1/2$: Thermal censorship

Is this hole –a geodesic incompleteness– an unavoidable feature of the bulk where CTCs are present? The previous analysis leads to this conclusion as long as α takes the same value in the upper patch as in the lower patch, where the choice was fixed by bulk regularity. However, once we have seen that the two bulk patches are disconnected spacetimes, only joined by the boundary metric, it would seem possible to choose, for a given Δ , a different value of α for each patch.

In effect, what this amounts to is to acknowledging that, since the quantum field is singular at the chronological Cauchy horizon, the states of the CFT on the two sides of the horizon need not be related. That is, the stress tensor function α need not be the same for $\tau^2 < 1$ and $\tau^2 > 1$. Could this allow to find a bulk dual for the upper patch such that, in spite of the CTCs, the state is free of other pathologies?

Since we may expect a horizon in the bulk, we look for a map between the metric (3.6) and that of Rindler-AdS₃ with periodically identified time,⁶

$$ds^2 = -(\hat{r}^2 - 1)d\hat{t}^2 + \frac{d\hat{r}^2}{\hat{r}^2 - 1} + \hat{r}^2 d\hat{\phi}^2. \quad (4.10)$$

This map is

$$\hat{t} = \frac{2\pi}{\Delta}\phi, \quad (4.11)$$

$$\hat{r}^2 = 1 + \left(\frac{\Delta}{2\pi}\right)^2 \frac{1}{z^2(\tau^2 - 1)} \left((1 - \tau^2) \left(1 + \frac{z^2}{4}\right) - \frac{\alpha}{2} z^2 \right)^2, \quad (4.12)$$

$$\hat{\phi} = \frac{\pi}{\Delta} \ln \left| \frac{1 + \tau}{1 - \tau} \right| - \operatorname{arctanh} \frac{z^2 - \left(\frac{\Delta}{\pi}\right)^2 \left(1 - \tau^2 - \frac{z^2}{4}\tau^2\right)}{\frac{\Delta}{\pi} z^2 \tau}, \quad (4.13)$$

where now

$$\alpha = \frac{1}{2} - \frac{2\pi^2}{\Delta^2}. \quad (4.14)$$

In accordance with (3.13), the horizon at $\hat{r} = 1$ is reached when

$$z = z_{\text{hor}} = \frac{\Delta}{\pi} \sqrt{\frac{\tau^2 - 1}{1 - \left(\frac{\Delta}{2\pi}\right)^2 \tau^2}}. \quad (4.15)$$

Upper patch. In the upper patch, with $\tau^2 > 1$, (4.12) implies that $\hat{r}^2 \geq 1$. However, if $\Delta > 2\pi$, corresponding to $0 < \alpha < 1/2$, the horizon at $\hat{r} = 1$ is never reached since z_{hor} is not real. That is, there is a hole in the space that removes the horizon, so again we have naked geodesic incompleteness.

Instead, if the time machine is slow, so $\Delta < 2\pi$, which implies $\alpha < 0$, the horizon is part of the bulk patch. In this case, the incompleteness of the hole is hidden by a horizon. The temperature of the horizon is $2\pi/\Delta$, i.e., the euclidean time periodicity is the same as the periodicity of the closed timelike curves. In CFT terms, by heating up the system to the correct temperature, we manage to (barely) restore the predictivity of the quantum theory and suppress the pathologies that the CTCs would induce. In other words, thermal censorship makes possible to have a CFT state compatible with the presence of CTCs.

⁶This is not a BTZ black hole if we do not require that $\hat{\phi}$ is periodic.

Lower patch. In the lower patch it is again convenient to rename the coordinates, now as

$$\hat{t} = \tilde{\varphi}, \quad \hat{\varphi} = \tilde{t}, \quad \hat{r}^2 = -\tilde{r}^2 + 1 \quad (4.16)$$

so (4.10) is now

$$ds^2 = -(\tilde{r}^2 - 1)d\tilde{t}^2 + \frac{d\tilde{r}^2}{\tilde{r}^2 - 1} + \tilde{r}^2 d\tilde{\varphi}^2, \quad (4.17)$$

with

$$\tilde{r}^2 = \left(\frac{\Delta}{2\pi}\right)^2 \frac{1 - \tau^2}{z^2} \left(1 + \frac{z^2}{4} - \frac{\alpha}{2} \frac{z^2}{1 - \tau^2}\right)^2 \quad (4.18)$$

(which is the same as r^2 in (4.3)). When $\tau^2 < 1$ and α is given by (4.14) there is a minimum value

$$\tilde{r}_{\min}^2 = 1 - \left(\frac{\Delta}{2\pi}\right)^2. \quad (4.19)$$

For all Δ this lies inside the horizon at $\tilde{r} = 1$. Since now $\tilde{\varphi}$ is the Killing direction that is periodically identified, outside this singularity we get the geometry of a BTZ black hole. As was the case for $\alpha > 1/2$, the time translation symmetry of the bulk is broken by the asymptotic boundary conditions. In this sense, then, the horizon of the black hole is not stationary.

When $\Delta < 2\pi$, so $\alpha < 0$, the minimum \tilde{r}_{\min} lies within the horizon and $\tilde{r} = 0$. Since $\tilde{r} = \tilde{r}_{\min}$ is a spacelike surface, the effect is that of having a spacelike singularity behind the horizon. Instead, when $\Delta > 2\pi$ and $0 < \alpha < 1/2$, there is no hole, but instead a conical singularity at $\tilde{r} = 0$.

5 Bulk dual for flat Misner spacetime

We have seen in Sec. 2.3 that we can recover the flat Misner spacetime as the near-chronological-horizon limit of Misner-AdS₂. We can apply the same limit to the CFT stress tensor. The anomalous trace disappears in flat space, but the traceless component of the stress tensor retains the form (3.3) in null coordinates (2.29).

We could now easily apply the bulk reconstruction procedure to this CFT state, but it is also straightforward to carry over all the results we have found for holographic Misner-AdS, taking the limits of the boundary metric and zooming in on small values of z by scaling

$$z \rightarrow \frac{z}{\sqrt{\epsilon}}. \quad (5.1)$$

The bulk metric we obtain is

$$ds^2 = \frac{1}{z^2} \left[dz^2 - \left(1 + \frac{\alpha^2}{4(X^+ X^-)^2} z^4\right) dX^+ dX^- - \frac{z^2}{2} \alpha \left(\left(\frac{dX^+}{X^+}\right)^2 + \left(\frac{dX^-}{X^-}\right)^2 \right) \right]. \quad (5.2)$$

The identifications are made along the orbits of the bulk Killing vector

$$k = X^- \frac{\partial}{\partial X^-} - X^+ \frac{\partial}{\partial X^+}, \quad (5.3)$$

with periodicity Δ . The action of the vector has fixed points at

$$z = \sqrt{\frac{2}{\alpha} X^+ X^-} \quad (5.4)$$

and the absence of conical singularities at these points requires that α is determined in terms of Δ by the same value (3.12) as before. These fixed points appear only in the region where $X^+ X^- > 0$, where there are no CTCs.

It is equally straightforward to find the coordinate changes from these metrics to global AdS₃ coordinates by taking the flat limit as described above⁷. The properties are qualitatively the same as in the case of the bulk duals of Misner-AdS₂ time machines: The bulk dual of the lower patch is in one-to-one correspondence with global AdS₃, while the upper patch is an infinitely multiple covering of it that does not contain the region inside the hole at

$$z \rightarrow 0, \quad T \rightarrow 0, \quad \frac{z^2}{2T} = \frac{\left(\frac{\Delta}{\pi}\right)^2}{1 + \left(\frac{\Delta}{2\pi}\right)^2}, \quad (5.5)$$

for which $r_{\min} = \bar{\Delta}$.

6 A stress-free time machine is dual to a bulk wormhole

Bulk wormhole. One possible bulk solution that has the same boundary geometry as we have been considering is (using again the proper distance coordinate $\sigma = \ln(2/z)$)

$$ds^2 = d\sigma^2 + \cosh^2 \sigma \left(-(d\tau + \tau d\psi)^2 + d\psi^2 \right) \quad (6.1)$$

with $\psi \sim \psi + \Delta$. This is indeed the same as the solution (3.5) for $\alpha = 0$, but it is actually a valid solution for any value of the periodicity Δ since there is no rotational fixed point that could fix it. In this state the traceless part of the stress tensor of the CFT vanishes

$$\langle \hat{T}_{ij} \rangle = 0 \quad (6.2)$$

(only the anomalous trace term remains), so, strikingly, the CFT is unexcited and remains in a stress-free state even if the spacetime evolves dynamically.

What is the interpretation of this stress-free state? The bulk geometry is completely regular (except for the presence of CTCs) and describes a traversable wormhole connecting two separate asymptotic regions at $\sigma \rightarrow +\infty$ and $\sigma \rightarrow -\infty$. At each constant- σ section we have a Misner-AdS₂ spacetime. During the time that CTCs are not present, the spatial topology of the bulk is that of a cylindrical wormhole, $\mathbb{R}_\sigma \times S_\psi^1$. Bear in mind that this bulk wormhole is completely unrelated to any wormhole that the Misner-AdS₂ spacetime may have originated from (see Sec. 8). It is, instead, the holographic description of a possible CFT state in the two-dimensional time machine spacetime.

But, taking the bulk viewpoint, the fact that we have managed to construct a traversable 3D wormhole without introducing any negative energies in the bulk should give us pause.

⁷It is also possible to find maps to Poincaré AdS₃ for $\alpha < 1/2$, see App. C.

This bulk is locally AdS₃ without any matter in it, but the results that forbid traversable wormholes are evaded by having CTCs. Observe that the time to cross the wormhole from one mouth to the other is $t = \pi$ (in units of AdS radius) which is longer than the time $t = 2$ that the spacetime without CTCs lasts. So it is impossible to cross the wormhole while remaining within a spacetime region that is free of CTCs.

Stress-free entangled CFT states. Since the bulk geometry has two different boundaries connected by a wormhole, we have two copies of the CFT in separate but identical 2D spacetimes. Then, the state of the CFT with $\langle \hat{T}_{ij} \rangle = 0$ is entangled with another CFT copy. Since a CFT in the circle has a ground-state negative Casimir energy, it would then seem that the energy of the degrees of freedom that entangle the two systems exactly cancels the Casimir energy. The entangled state might seem similar to a thermofield double state, but this cannot be entirely correct since the thermofield double is dual to a non-traversable wormhole.

It seems that (6.1), even though completely non-singular, is a very fragile state. The addition of any positive energy will presumably close the bulk wormhole by turning it into a BTZ black hole. Also, if we stop the time-shifting effect before the appearance of CTCs, the bulk will turn into a massless BTZ black hole in which one of the mouths of the wormhole closes to zero size.

Finally, for the flat Misner spacetime one can also construct a holographic bulk dual of a stress-free state. It is

$$ds^2 = \frac{1}{z^2} (dz^2 - d\psi (2dT + Td\psi)) , \quad (6.3)$$

with periodically identified ψ . The holographic stress-energy tensor in (6.3) vanishes, but now the bulk geometry does not describe a wormhole. Instead, the z -cylinder ends at an orbifold singularity at $z \rightarrow \infty$. In this respect, the stress-free state (6.1) in Misner-AdS₂ is better behaved. Interestingly, for a *free* CFT in a flat Misner spacetime, it was found in [12, 13] that there are states for which the stress tensor vanishes (they also find states with \hat{T}_{\pm} like (3.3)). The claim in [13] is that these states are ill defined on the Cauchy horizon. In [12], they conclude that the divergence is in a set of measure zero. These conclusions seem to fit well with the presence of a null orbifold singularity in the bulk dual (6.3).

7 Euclidean analysis

In order to deduce the correct bulk interpretation for the time machine dual, we need to determine the preferred state of the boundary CFT. Therefore, we can compare the free energies associated to two states of the CFT: one with zero stress tensor and another with a natural stress tensor, as computed by Frolov in [5], and additionally extended to strong coupling via holography as we have done above. In order to make the analysis as clear as possible, we will compare the free energies only for the upper, CTC region; the lower region is time-dependent and it is not clear if a thermodynamic analysis can be applied.

First, we focus on the solution which is sourced by the stress tensor (3.3), that is,

$$ds^2 = \frac{\ell^2}{z^2} \left[dz^2 - \left(1 + \frac{z^2}{4} + \frac{\alpha}{2} z^2 \sinh^2 \xi \right)^2 \frac{d\bar{t}^2}{\sinh^2 \xi} + \left(1 + \frac{z^2}{4} - \frac{\alpha}{2} z^2 \sinh^2 \xi \right)^2 \frac{d\xi^2}{\sinh^2 \xi} \right]. \quad (7.1)$$

We have introduced the coordinate

$$\xi = \operatorname{arccoth} \tau \quad (7.2)$$

which is convenient for the restriction to the upper patch, and we have renamed $\phi = \bar{t}$, as it is a timelike coordinate in this patch.

We follow [14] for the Euclidean analysis and the determination of necessary counterterms, which in three dimensions gives

$$I_E(g) = -\frac{1}{16\pi} \int_{\mathcal{M}} \sqrt{g} (R - 2\Lambda) - \frac{1}{8\pi} \int_{\partial\mathcal{M}} \sqrt{h} K + \frac{1}{8\pi\ell} \int_{\partial\mathcal{M}} \sqrt{h}, \quad (7.3)$$

where g , R and Λ are associated to the bulk spacetime, h and K to the boundary one, and $\Lambda = -\frac{1}{\ell^2}$. In (7.1), time is represented by the coordinate \bar{t} , which after euclideanizing, $i\bar{t} = \bar{\tau}$, is still periodically identified as $\bar{\tau} \sim \bar{\tau} + \Delta$. The coordinate ξ takes all real values, $\xi \in (-\infty, \infty)$, while $z \in (0, \infty)$. For the calculation of the Euclidean action, we use $\xi \in (-\xi_0, \xi_0)$, where $\xi_0 \rightarrow \infty$, and $z \in (\epsilon, z_0)$, where $\epsilon \rightarrow 0$ and $z_0 \rightarrow \infty$. Since we have two boundaries, $z = z_0$ and $z = \epsilon$, we will need two counterterms associated with them, as well as the boundary terms⁸.

The final result for the action is pretty simple,

$$I_E(g_\alpha) = -\frac{\Delta\ell}{4\pi} (1 + \alpha/2 - \log \epsilon + \log z_0), \quad (7.4)$$

where the log terms come from the conformal anomaly of the boundary metrics; they naturally appear in the stress-free calculation as well, so we can neglect them. When computing the action, a subtlety arises when we take two limits: $\epsilon \rightarrow 0$ and $\xi_0 \rightarrow \infty$. The term that arises is proportional to

$$\epsilon^2 (\xi_0 - \sinh 2\xi_0), \quad (7.5)$$

so we see that we have to be careful. Since we found a hole with minimum size in this patch, we can deduce what is the correct limit value. The limit (4.8), for $z \rightarrow 0$ and $\xi \rightarrow \infty$ is

$$z \sinh \xi = \sqrt{\frac{2}{\alpha}}. \quad (7.6)$$

Since ξ goes to ∞ , we see that the z going to 0 competes with an exponential in ξ ; in other words, z reaches 0 very fast. Therefore, the product $z\xi$ goes to 0. Note also that we have in (7.5) z^2 multiplying $\sinh 2\xi$. In the limit of large ξ , this product becomes quadratic, $(ze^\xi)^2$, and so, we can apply (7.6), just adjusting for factors of 2.

⁸One caveat to keep in mind is the sign of the normal vector n^z : it will change sign depending on whether it is normal inwards (as in the case of $z = \epsilon$) or outwards ($z = z_0$).

As for the stress-free bulk, the metric is given by (7.1) just with $\alpha = 0$, and so,

$$ds^2 = \frac{\ell^2}{z^2} \left[dz^2 + \text{csch}^2 \xi (1 + z^2/4)^2 (-d\bar{t}^2 + d\xi^2) \right]. \quad (7.7)$$

The calculation is fairly similar, just without any subtleties with limits, so the final result is given by

$$I_E(g_0) = -\frac{\Delta\ell}{4\pi} (1 - \log \epsilon + \log z_0). \quad (7.8)$$

We see that this action is almost the same as the previous one given in (7.4), except for one term which depends on α .

We see that both actions depend linearly on Δ , indicating that the entropy of these spacetimes is 0. However, we can compute their (free) energies, and we obtain (neglecting log terms)

$$F_\alpha = E_\alpha = \partial_\Delta I_E(g_\alpha) = -\frac{\ell}{4\pi} (1 + \alpha/2), \quad (7.9)$$

$$F_0 = -\frac{\ell}{4\pi}. \quad (7.10)$$

We clearly see that F_α dominates unless $\alpha < 0$. As seen from previous discussions, $\alpha < 0$ corresponds to Rindler-AdS. And so, we come to the conclusion that the hole will dominate over stress-free empty spacetime, unless we form Rindler-AdS, in which case the dominant geometry is the stress-free bulk. Therefore, in a spacetime with CTCs, geodesic incompleteness is preferred over empty, CTC-filled spacetimes.

8 Time machines from wormholes

As we mentioned in Sec. 1, time machines seem to be a generic feature of traversable wormholes. We will show in [15] that this conclusion is premature, but the connection gives a physical motivation for studying their properties, so we will explain it here. We follow previous literature [5], but highlight the connection to the Misner-AdS geometry which, to our knowledge, had not been made before.

The geometry of a spherically symmetric wormhole can be written in the form

$$ds^2 = -e^{-2\Phi(\lambda)} dt^2 + d\lambda^2 + R^2(\lambda) d\Omega_2, \quad (8.1)$$

where we take $R(\lambda)$ to be a U-shaped function of $\lambda \in (-\infty, +\infty)$, with $R^2 \rightarrow \lambda^2$ as $|\lambda| \rightarrow \infty$. The mouths are where the behavior $R \simeq |\lambda|$ sets in. In (8.1) the two mouths live in different asymptotic regions, but we will want them connected within the same space, so that it is possible travel between them through the ‘exterior’ universe. This necessarily breaks the spherical symmetry of (8.1), but we will still consider it to be a good approximation near each of the mouths. We do not assume that the tube is short, neither compared to its characteristic radius nor to the exterior distance between mouths.

The gravitational potential $\Phi(\lambda)$ is finite everywhere, so there are no horizons and the wormhole is traversable. We assume that $\Phi(\lambda) \rightarrow \Phi_\infty^\pm$ as $\lambda \rightarrow \pm\infty$. Typically, these asymptotic values are reached not far from the mouths.

For our present discussion, we will not specify the gravitational theory and the matter that support this geometry. But we must bear in mind that having a self-consistent model of a wormhole is crucial for deciding what constraints exist on the features, such as the length, of a physically allowed wormhole. It is also necessary for examining its stability and its reaction to attempts to turn it into a time machine, as we will do in [15].

In order to create a time machine, we set the two mouths at different gravitational potentials, $\Phi_{\infty}^+ \neq \Phi_{\infty}^-$, e.g., by placing a heavy object near one of the mouths. Then, a time-shift will grow between the two sides. A particle traveling in a circular trajectory along the wormhole will experience a net gravitational force and will get accelerated, gaining or losing energy along the way, so this is a non-potential gravitational field.

Say that, before introducing any redshift between the two mouths, L_{wh} is the asymptotic exterior time that a light ray takes to cross the wormhole tube joining two chosen points near each of the mouths, and d_{out} is the time in which a light ray travels between the same two points across the outside universe. Then, a chronology horizon appears when the redshifting effect has been operating for an asymptotic time⁹

$$T_{\text{CH}} = \frac{L_{\text{wh}} + d_{\text{out}}}{|\Phi_{\infty}^+ - \Phi_{\infty}^-|}. \quad (8.2)$$

At any later time, a time machine is present. Notice that this does not require that the wormhole we started with is short, in the sense that $L_{\text{wh}} < d_{\text{ext}}$. If we begin with a very long wormhole, we simply have to wait a correspondingly long time to form the time machine. Of course, as the redshift operates, the wormhole becomes shorter in the sense that time to cross the wormhole, measured by an exterior observer, gets smaller (in one direction – in the other it gets bigger). But, to the extent that one can make a distinction between exterior and interior,¹⁰ the proper length of the wormhole tube can still remain much longer than the outside separation between the mouths.

An important assumption in this argument is that, as we mentioned before, the wormhole spacetime geometry remains fixed throughout, and in particular is not affected by the quantum energy fluxes induced by the time-dependent geometry (which we have computed), even when these become large. In this article we will not dwell further on this matter.

Wormhole time machine as Misner-AdS

We now make a simplification and study the 1 + 1 geometry seen by a particle, or a field excitation, traveling in a circle along the wormhole. Such a restriction is well justified when the field excitation is constrained to move along such lines, as is the case in the magnetic-line model of [16] or in the cosmic string model of [17]. In other cases, the model may miss relevant features due to propagation in directions transverse to these worldlines [4], but any rate, the truncation allows to develop a useful ‘standard wormhole time machine model’. Fixing the angle on the sphere in (8.1) gives

$$ds^2 = -e^{-2\phi(\lambda)} dt^2 + d\lambda^2, \quad (8.3)$$

⁹For simplicity we are assuming a small redshifting effect, so that $e^{\Phi_{\infty}^+ - \Phi_{\infty}^-} \simeq 1 + \Phi_{\infty}^+ - \Phi_{\infty}^-$.

¹⁰In general, such a distinction is not precisely defined.

where points along λ are periodically identified, $\lambda \sim \lambda + L_\lambda$, with L_λ the total length of the wormhole circle. For a typical wormhole, the redshift ϕ grows in the interior of the throat reaching a maximum at its middle.

To make a time machine, we assume that $\phi(0) \neq \phi(L_\lambda)$. The time coordinates t at $\lambda = 0$ and t' at $\lambda = L_\lambda$ must then be related by

$$e^{-\phi(L_\lambda)}t' = e^{-\phi(0)}t, \quad (8.4)$$

or equivalently, we identify the spacetime points

$$(t, 0) \sim (e^{-\phi(0)+\phi(L_\lambda)}t, L_\lambda). \quad (8.5)$$

The spacetime (8.3) can always be Weyl-transformed to the form

$$ds^2 = -e^{-2a\psi}dt^2 + d\psi^2, \quad (8.6)$$

with constant a , by a conformal change of coordinates $\lambda \rightarrow \psi$ that, importantly, does not involve t . This transformation uniformizes the path, while retaining the growing time shift between the mouths. The new geometry, which [5] referred to as the ‘standard model’, is locally the same as the Poincaré metric in AdS₂ with curvature radius $1/a$, but now with points identified in such a way that

$$(t, \psi) \sim (e^{aL}t, \psi + L), \quad (8.7)$$

where L is the new periodicity of ψ . The coordinate t here is actually the same as in (2.8). Then, if we change

$$t = \tau e^{a\psi} \quad (8.8)$$

the geometry (8.6) becomes the same, locally and globally, as the Misner-AdS₂ spacetime of (2.5). The appearance of CTCs in this model is in direct correspondence with that in the original wormhole, (8.2).

9 Discussion

Let us summarize the main findings in this paper. We have established a holographic correspondence between a CFT on a time machine background and its associated bulk dual. On the boundary side, closed timelike curves are developed at some point, splitting the spacetime into two parts: one without CTCs (lower patch) and another with CTCs (upper patch). These patches are separated by a Cauchy horizon, which in this case is a chronology horizon as well. The analysis of quantum fields in this spacetime leads to a divergent stress tensor at the chronology horizon [5], and it has been proposed that this forbids the passage to the pathological part of the spacetime [2–5, 7, 13]. The dual bulk side demonstrates this form of chronology protection in a compelling and subtle manner: The bulk geometry is separated into two patches, with and without CTCs, but, since the spacetime is locally equivalent to AdS₃, its curvature is constant and cannot exhibit any divergence. The separation is nevertheless as drastic as can be. The lower (no-CTC)

spacetime is a geodesically complete, global AdS₃ geometry totally disconnected from the upper (CTC) region; they are only connected through the boundary where the chronology horizon lies. Such a separation clearly indicates that no finite energy excitation can ever cross to the region with CTCs, thereby manifestly enforcing the chronology protection.

One might wonder how we can say anything *at all* about the upper patch, given that a divergent stress tensor develops beforehand. Indeed, it was emphasized in [18] that one cannot make meaningful predictions about the state of the quantum fields beyond a Cauchy horizon (nor about the spacetime itself)¹¹. Simply put, we cannot pose an initial value problem on a singular slice, although we can put initial values on a slice just beyond it. However, these initial values can be chosen completely independently of the state before the Cauchy horizon. In the bulk construction, this is manifest since the lower-patch bulk is geodesically complete and therefore cannot affect anything “outside” its domain of dependence.

Nevertheless, we can certainly discuss the possible states of the CFT in the upper patch and their bulk duals; these states might not make sense beyond a singular Cauchy horizon, but they can be analyzed as independently prepared states with no ties to the lower patch, as we have done in Sec. 3. Our results are summarized in Tab. 1.

	CFT state	Lower patch	Upper patch
$\alpha < 0$	thermal	BTZ black hole	Rindler-AdS ₃
$\alpha = 0$	zero-energy	bulk traversable wormhole	
$0 < \alpha < 1/2$	Casimir + thermal (?)	BTZ black hole	hole in AdS ₃
$\alpha > 1/2$	Casimir	global AdS ₃	hole in AdS ₃

Table 1: Summary of our results for various values of α , which determines the CFT stress tensor (3.3). The lower patch has no CTCs, but the upper patch has them. For $\alpha > 1/2$, the lower patch is regular, while the upper patch develops geodesic incompleteness. For $\alpha < 0$, the stress tensor is thermally dominated and there is a horizon in the bulk; in the lower patch it is a BTZ black hole, while in the upper patch it is a Rindler horizon, associated to an accelerated observer (the boundary). The case of $\alpha \in (0, 1/2)$ also leads to a BTZ black hole in the lower patch, and in the upper region it gives rise to a hole not hidden by a horizon. The stress tensor in this regime is presumed to be a combination of Casimir and thermal effects. Finally, we have the case of $\alpha = 0$, which sets the bulk to a two-sided wormhole, as explained in Sec. 6.

Given that the hole remains as a generic feature of CTC boundaries, one can ask about its interpretation in the context of holography¹². For instance, we see that the bulk reconstruction fails to encompass the entire bulk spacetime – can we interpret this in the context of quantum error correcting codes, that is, tensor networks? One might try

¹¹Note that, in variance with the conclusions, and therefore, the title, of [18], we argued in [19] that the BTZ black hole does not violate the strong cosmic censorship once we include sufficiently high loop corrections to the spacetime.

¹²One might have thought that the results of [20] have implications for our work here. However, note that the hole in our setup is due to geodesic incompleteness, and it does not carry any entropy (as can be seen from the Euclidean analysis in Sec. 7).

to connect these results to the existence of an end-of-the-world (EoW) brane, for which the bulk also exhibits hole-like features [21]. However, the EoW brane carries boundary conditions with it, and while it does cut-off the spacetime, it does so in an induced manner; in other words, the brane can carry degrees of freedom and have entropy – our hole has neither of these features. Another way of probing the hole is to evaluate its complexity, which may be identified with some measure of volume in the bulk. If we start from the lower patch and try to evolve across the Cauchy horizon, we see that the volume of the lower patch eventually ends up being zero – the bulk disconnects from the upper patch, and hence the volume shrinks to zero size. The singularity in the CFT that separates the two states would then seem to involve a reduction in complexity.

Finally, let us briefly mention how backreaction effects of the CFT on the background geometry might alter the picture we have presented in this paper. Could backreaction open a bulk passage between the two disconnected patches? We believe this is unlikely since, as we will explain in [15], in a wormhole time machine the achronal averaged null energy condition, which is supposed to be satisfied by physical quantum matter, implies that significant changes in the spacetime must occur well before the chronological horizon is reached, which will prevent the appearance of CTCs. It seems much more likely that when backreaction is included, the mild behavior of the CFT that we have found in the lower patch gets extended to all times. In our holographic model, the study of CFT backreaction could be implemented through braneworld holography.

Acknowledgments

We thank Tomás Andrade, Evan Coleman, and Mikel Sánchez-Garitaonandia for useful discussions. Work supported by ERC Advanced Grant GravBHs-692951, MICINN grants FPA2016-76005-C2-2-P and PID2019-105614GB-C22, and AGAUR grant SGR-2017-754. We also acknowledge financial support from the State Agency for Research of the Spanish Ministry of Science and Innovation through the “Unit of Excellence María de Maeztu 2020-2023” award to the Institute of Cosmos Sciences (CEX2019-000918-M).

A Hyperboloidal embeddings

In this section, we rewrite our main AdS₂ metrics in terms of the embedding coordinates; such transformations are useful when discussing different patches of the boundary and bulk patches.

The Misner-AdS₂ spacetime metric (2.5) (with $a = 1$) can be obtained from the hyperboloid

$$ds^2 = -dV^2 - dW^2 + dX^2, \quad -V^2 - W^2 + X^2 = -1, \quad (\text{A.1})$$

by making

$$\begin{aligned} V + X &= e^{-\psi}, \\ V - X &= e^{\psi}(1 - \tau^2), \\ W &= \tau. \end{aligned} \quad (\text{A.2})$$

These coordinates cover $V + X > 0$. The identification is

$$V \pm X \sim e^{\mp\Delta}(V \pm X), \quad (\text{A.3})$$

which is an AdS_2 boost. This spacetime can then also be obtained by going to Rindler coordinates and identifying along the boost. Maintaining the τ coordinate and changing ψ to another periodic coordinate ϕ , such that

$$V \pm X = \sqrt{1 - \tau^2} e^{\mp\phi}, \quad W = \tau, \quad (\text{A.4})$$

we recover the metric (2.25).

Misner-AdS₃

Finally, let us briefly discuss the Misner-AdS₃ spacetime, with metric

$$ds^2 = -(d\tau + \tau d\psi)^2 + (dy + y d\psi)^2 + d\psi^2, \quad (\text{A.5})$$

and identifications

$$(\tau, y, \psi) \sim (\tau, y, \psi + \Delta), \quad (\text{A.6})$$

such that CTCs appear when $\tau^2 > 1 + y^2$. This is embedded in the hyperboloid

$$-V^2 - W^2 + X^2 + Y^2 = -1, \quad ds^2 = -dV^2 - dW^2 + dX^2 + dY^2, \quad (\text{A.7})$$

by making

$$V^+ = V + X = e^\psi, \quad (\text{A.8})$$

$$V^- = V - X = e^{-\psi} (1 - \tau^2 + y^2), \quad (\text{A.9})$$

$$W = \tau, \quad (\text{A.10})$$

$$Y = y. \quad (\text{A.11})$$

Periodic identifications of ψ are identifications along orbits of the boost vector

$$X\partial_V + V\partial_X = V^+\partial_{V^+} + V^-\partial_{V^-}. \quad (\text{A.12})$$

These are the same identifications as in the static BTZ black hole [22]. The geometry has an orbifold singularity at the fixed point set of the boost action. In the static BTZ black hole one retains the region where the boost action remains spacelike and therefore there are no CTCs, but in Misner-AdS₃ one does the opposite.

More relevantly for us, the boundary geometry of Misner-AdS₃ is not a Misner-AdS₂ geometry, but instead 2D Minkowski spacetime with periodically identified time. The chronology horizon of Misner-AdS₃ lies entirely in the bulk, and does not intersect the boundary. Then, Misner-AdS₃ does not constitute a possible holographic bulk dual for the CFT in Misner-AdS₂.

B Bulk reconstruction in AdS₃

We will follow [11], where it is shown that in an AdS₃ bulk the Fefferman-Graham expansion truncates exactly to the form

$$ds^2 = \frac{\ell^2}{z^2} \left(dz^2 + \left(g_{ij} + z^2 g_{ij}^{(2)} + \frac{z^4}{4} g^{(2),k} g_{kj}^{(2)} \right) dx^i dx^j \right). \quad (\text{B.1})$$

Indices are raised and lowered with the boundary metric g_{ij} (we omit the index (0)). The term $g_{ij}^{(2)}$ determines the stress tensor as

$$g_{ij}^{(2)} = \frac{1}{2} (t_{ij} - Rg_{ij}), \quad (\text{B.2})$$

where R is the scalar curvature of g_{ij} and t_{ij} is the ‘geometric stress tensor’, which satisfies

$$\nabla_i t^{ij} = 0, \quad t^i{}_i = R, \quad (\text{B.3})$$

and yields the physical holographic stress tensor as

$$T_{ij} = \frac{\ell}{16\pi G} t_{ij} = \frac{c}{24\pi} t_{ij}. \quad (\text{B.4})$$

It is often convenient to separate its traceless part,

$$\hat{t}_{ij} = t_{ij} - \frac{1}{2} Rg_{ij}, \quad (\text{B.5})$$

in terms of which

$$g_{ij}^{(2)} = \frac{1}{2} \left(\hat{t}_{ij} - \frac{1}{2} Rg_{ij} \right). \quad (\text{B.6})$$

Now we insert this into (B.1) to obtain

$$ds^2 = \frac{\ell^2}{z^2} \left[dz^2 + \left[\left(\left(1 - \frac{R}{8} z^2 \right)^2 + \frac{\hat{t}^2}{32} z^4 \right) g_{ij} + \frac{z^2}{2} \left(1 - \frac{R}{8} z^2 \right) \hat{t}_{ij} \right] dx^i dx^j \right], \quad (\text{B.7})$$

where we denote

$$\hat{t}^2 \equiv \hat{t}^{ij} \hat{t}_{ij}, \quad (\text{B.8})$$

and we have used that

$$\hat{t}_i{}^k \hat{t}_{kj} = \frac{\hat{t}^2}{2} g_{ij}. \quad (\text{B.9})$$

Now consider the case where the boundary metric is written in null coordinates $x^\pm = t \pm x$ as

$$g_{ij} dx^i dx^j = -g(x^+, x^-) dx^+ dx^- \quad (\text{B.10})$$

so that $g_{+-} = -g/2$, $g^{+-} = -2/g$, and

$$\hat{t}_{ij} dx^i dx^j = \hat{t}_+ (dx^+)^2 + \hat{t}_- (dx^-)^2, \quad (\text{B.11})$$

$$\hat{t}^2 = \frac{8}{g^2} \hat{t}_+ \hat{t}_-. \quad (\text{B.12})$$

Then

$$ds^2 = \frac{\ell^2}{z^2} \left[dz^2 - \left(\left(1 - \frac{R}{8} z^2 \right)^2 g + \frac{\hat{t}_+ \hat{t}_-}{4g} z^4 \right) dx^+ dx^- + \frac{z^2}{2} \left(1 - \frac{R}{8} z^2 \right) \left(\hat{t}_+ (dx^+)^2 + \hat{t}_- (dx^-)^2 \right) \right]. \quad (\text{B.13})$$

The BTZ black hole is recovered for $g_{ij} = \eta_{ij}$ (so $R = 0$) and constant $\hat{t}_{tt} = \hat{t}_{xx} = \mu$; in null coordinates, this is $g = 1$, and $\hat{t}_+ = \hat{t}_- = \mu/2$. The dimensionless constant is $\mu = 8GM$. For $\mu = -1$ we recover global AdS₃.

Apply this to the Misner-AdS₂ spacetime, which as we have seen in Sec. 2.2 is a quotient of the Poincaré AdS₂ geometry, with

$$g = \frac{4}{(x^+ - x^-)^2} \quad (\text{B.14})$$

(so that $R = -2$), and with the traceless stress tensor (3.3),

$$\hat{t}_{\pm} = -\frac{\alpha}{(x^{\pm})^2} \quad (\text{B.15})$$

which is conserved when α is constant. Substituting in (B.13) we obtain the bulk metric (3.5). If, instead, we take $g = 1$ with the same stress tensor, we find (5.2).

C Mapping the flat-Misner bulk to Poincaré AdS₃

Let us see how the spacetime (5.2) can be obtained by a coordinate transformation from Poincaré AdS₃,

$$ds^2 = \frac{\ell^2}{\tilde{z}^2} (d\tilde{z}^2 - d\tilde{y}^+ d\tilde{y}^-). \quad (\text{C.1})$$

Observe first that, in the boundary theory, the change

$$y^{\pm} = (X^{\pm})^{\gamma} \quad (\text{C.2})$$

generates, through the Schwarzian,

$$\hat{t}_{\pm} = -\{y^{\pm}, X^{\pm}\}, \quad (\text{C.3})$$

the stress tensor (B.15) with

$$\alpha = \frac{1 - \gamma^2}{2}. \quad (\text{C.4})$$

The bulk change of coordinates that reproduces this transformation can be obtained from, e.g., [23], to find

$$y^{\pm} = (X^{\pm})^{\gamma} \frac{X^+ X^- + (\gamma^2 - 1)z^2/4}{X^+ X^- - (\gamma - 1)^2 z^2/4}, \quad \tilde{z} = z \frac{\gamma (X^+ X^-)^{\frac{\gamma+1}{2}}}{X^+ X^- - (\gamma - 1)^2 z^2/4}. \quad (\text{C.5})$$

When $\gamma = 0$ we get an invalid coordinate change, but this can be corrected by taking an appropriate limit. Then, the change of coordinates,

$$\begin{aligned} y^\pm &= \ln x^\pm - \frac{z^2/2}{X^+ X^- - z^2/4}, \\ \tilde{z} &= z \frac{\sqrt{X^+ X^-}}{X^+ X^- - z^2/4} \end{aligned} \tag{C.6}$$

gives to (5.2) with $\alpha = 1/2$, which is indeed the value that obtains from the Schwarzian stress tensor in the boundary when changing $y^\pm = \ln X^\pm$.

This change of coordinates can be obtained as a limit of the ones we introduced for Misner-AdS₂ for $\alpha < 1/2$.

References

- [1] N. Graham and K. D. Olum, “Achronal averaged null energy condition,” *Physical Review D* **76** no. 6, (Sep, 2007) . <http://dx.doi.org/10.1103/PhysRevD.76.064001>.
- [2] S. W. Hawking, “Chronology protection conjecture,” *Phys. Rev. D* **46** (Jul, 1992) 603–611. <https://link.aps.org/doi/10.1103/PhysRevD.46.603>.
- [3] M. S. Morris, K. S. Thorne, and U. Yurtsever, “Wormholes, Time Machines, and the Weak Energy Condition,” *Phys. Rev. Lett.* **61** (1988) 1446–1449.
- [4] M. Visser, *Lorentzian wormholes: From Einstein to Hawking*. 1995.
- [5] V. P. Frolov, “Vacuum polarization in a locally static multiply connected spacetime and a time-machine problem,” *Phys. Rev. D* **43** (Jun, 1991) 3878–3894. <https://link.aps.org/doi/10.1103/PhysRevD.43.3878>.
- [6] I. Arefeva, A. Bagrov, P. Säterskog, and K. Schalm, “Holographic dual of a time machine,” *Physical Review D* **94** no. 4, (Aug, 2016) . <http://dx.doi.org/10.1103/PhysRevD.94.044059>.
- [7] B. S. Kay, M. J. Radzikowski, and R. M. Wald, “Quantum Field Theory on Spacetimes with a Compactly Generated Cauchy Horizon,” *Communications in Mathematical Physics* **183** no. 3, (Feb, 1997) 533–556. <http://dx.doi.org/10.1007/s002200050042>.
- [8] S. H. 60th Birthday Workshop, E. Symposium (2002, Cambridge, S. Hawking, G. Gibbons, StephenHawking, P. Shellard, E. Shellard, E. Cambridge Stephen Hawking 60th Birthday Conference 2002, S. Rankin, C. U. Press, U. of Cambridge. Centre for Mathematical Sciences, *et al.*, *The Future of Theoretical Physics and Cosmology: Celebrating Stephen Hawking’s Contributions to Physics*. Cambridge University Press, 2003. <https://books.google.com.pr/books?id=yLy4b61rfPwC>.
- [9] L.-X. Li, “Time machines constructed from anti-de Sitter space,” *Physical Review D* **59** no. 8, (Mar, 1999) . <http://dx.doi.org/10.1103/PhysRevD.59.084016>.
- [10] C. W. Misner, “Taub-NUT space as a counterexample to almost anything.”
- [11] S. de Haro, K. Skenderis, and S. N. Solodukhin, “Holographic Reconstruction of Spacetime and Renormalization in the AdS/CFT Correspondence,” *Communications in Mathematical Physics* **217** no. 3, (Mar, 2001) 595–622. <http://dx.doi.org/10.1007/s002200100381>.
- [12] L.-X. Li and J. R. Gott, “Self-Consistent Vacuum for Misner Space and the Chronology Protection Conjecture,” *Physical Review Letters* **80** no. 14, (Apr, 1998) 2980–2983. <http://dx.doi.org/10.1103/PhysRevLett.80.2980>.
- [13] C. R. Cramer and B. S. Kay, “Thermal and two-particle stress-energy must be ill defined on the two-dimensional Misner space chronology horizon,” *Physical Review D* **57** no. 2, (Jan, 1998) 1052–1056. <http://dx.doi.org/10.1103/PhysRevD.57.1052>.
- [14] R. Emparan, C. V. Johnson, and R. C. Myers, “Surface terms as counterterms in the AdS-CFT correspondence,” *Physical Review D* **60** no. 10, (Oct, 1999) . <http://dx.doi.org/10.1103/PhysRevD.60.104001>.
- [15] R. Emparan and M. Tomašević, “Time in traversable wormholes,” in preparation, 2021.
- [16] J. Maldacena, A. Milekhin, and F. Popov, “Traversable wormholes in four dimensions,” 2020.

- [17] Z. Fu, B. Grado-White, and D. Marolf, “Traversable Asymptotically Flat Wormholes with Short Transit Times,” *Class. Quant. Grav.* **36** no. 24, (2019) 245018, [arXiv:1908.03273 \[hep-th\]](#).
- [18] O. J. C. Dias, H. S. Reall, and J. E. Santos, “The BTZ black hole violates strong cosmic censorship,” *JHEP* **12** (2019) 097, [arXiv:1906.08265 \[hep-th\]](#).
- [19] R. Emparan and M. Tomašević, “Strong cosmic censorship in the BTZ black hole,” *JHEP* **06** (2020) 038, [arXiv:2002.02083 \[hep-th\]](#).
- [20] V. Balasubramanian, B. D. Chowdhury, B. Czech, J. de Boer, and M. P. Heller, “Bulk curves from boundary data in holography,” *Physical Review D* **89** no. 8, (Apr, 2014) .
<http://dx.doi.org/10.1103/PhysRevD.89.086004>.
- [21] M. V. Raamsdonk, “Building up spacetime with quantum entanglement II: It from BC-bit,” 2018.
- [22] M. Banados, M. Henneaux, C. Teitelboim, and J. Zanelli, “Geometry of the (2+1) black hole,” *Phys. Rev. D* **48** (1993) 1506–1525, [arXiv:gr-qc/9302012](#). [Erratum: Phys.Rev.D 88, 069902 (2013)].
- [23] M. M. Roberts, “Time evolution of entanglement entropy from a pulse,” *JHEP* **12** (2012) 027, [arXiv:1204.1982 \[hep-th\]](#).